

Protection from Doxorubicin-Induced Cardiac Toxicity in Mice with a Null Allele of Carbonyl Reductase 1¹

Lisa E. Olson, Djahida Bedja, Sara J. Alvey, A. J. Cardounel, Kathleen L. Gabrielson, and Roger H. Reeves²

Johns Hopkins University School of Medicine, Department of Physiology, Baltimore, Maryland 21205 [L. E. O., R. H. R.]; Johns Hopkins University School of Medicine, Department of Comparative Medicine, Baltimore, Maryland 21287 [D. B., S. J. A., K. L. G.]; and Heart and Lung Research Institute, Ohio State University, Columbus, Ohio 43210 [A. J. C.]

ABSTRACT

Doxorubicin is a highly effective antineoplastic agent, but it can produce the serious side effects of acute cardiac injury and chronic congestive heart failure. Carbonyl reductase (CBR) has been implicated in the development of doxorubicin-induced cardiotoxicity. To test whether a decrease in CBR levels was protective against doxorubicin toxicity, we created a null allele of the *Cbr1* gene. Mice with one functional copy of the gene (*Cbr1* +/-) were healthy and grossly normal despite having decreased levels of *Cbr1* transcript and protein. Control and *Cbr1* +/- mice were administered doxorubicin at 20 mg/kg i.p. *Cbr1* +/- mice showed decreased circulating levels of the cardiotoxic metabolite, doxorubicinol, after administration. Within 2 weeks, 91% of wild-type mice were severely affected ($n = 11$) compared with 18% of *Cbr1* +/- mice ($n = 11$). Echocardiography and histological analysis showed that *Cbr1* +/- mice were protected from gross and cellular level pathologies associated with doxorubicin treatment. Demonstration that inhibition of carbonyl reductase blocks the toxic effects on the heart has important implications for improving the use of doxorubicin in chemotherapy.

INTRODUCTION

Doxorubicin is a common chemotherapeutic drug used to treat solid and hematopoietic tumors. Its use is limited by the major side effect of cardiac toxicity (1), which has not been effectively prevented by pharmacologic intervention with cardioprotective drugs (2, 3). The mechanism by which doxorubicin or its metabolites cause chronic cardiomyopathy is not fully understood. Hypotheses regarding the mechanism of cardiac toxicity include perturbation of calcium homeostasis, formation of iron complexes, generation of radical oxygen species, mitochondrial dysfunction, and damage to cell membranes (4).

CBR1³ (EC 1.1.1.184) is a member of the short chain dehydrogenase/reductase family and reduces many carbonyl substrates to alcohols (5). CBR1 has been shown to be the major reductase in mouse kidney, spleen, and heart (6), but is produced at a low level in every tissue examined (data not shown). The gene contains three exons and produces a 1.2 kb mRNA. The CBR1 protein is monomeric and found in the cytoplasm (5, 7). The gene encoding CBR1 (*CBR1*) is found on human chromosome 21, and its murine orthologue (*Cbr1*) is on mouse chromosome 16. A highly homologous carbonyl reductase gene, *Cbr3*, is located adjacent to *Cbr1* in both mice and humans, and is 84% identical to CBR1 at the protein level (7). Evidence for transcription of *Cbr3* in mouse exists (8, 9), but enzyme activity has not been described. An extra copy of both genes is present in individuals with trisomy 21 (Down syndrome). CBR2, which is not evolutionarily conserved with CBR1 and CBR3, is tetrameric, expressed in the

mitochondria of the lung (5), and maps to mouse chromosome 11 (10).

CBR1 catalyzes the reduction of doxorubicin to doxorubicinol, the suspected toxic metabolite involved in chronic heart toxicity (11). Transgenic mice that overexpress human CBR1 exclusively in the heart show increased heart damage and decreased survival after doxorubicin treatment (12). However, these mice exhibit CBR1 activity at 470-fold higher levels than wild-type mice, and, thus, do not reflect physiological conditions.

We hypothesized that a decrease in CBR1 would limit doxorubicin-induced cardiotoxicity. Given multiple enzymes with potential carbonyl reductase activity, it is important to demonstrate that specifically lowering CBR1 activity is relevant to ameliorating doxorubicin toxicity. Our results show that the loss of one copy of *Cbr1* is sufficient to protect mice from this cardiac pathology. Thus, diminution of CBR1 activity using pharmacologic inhibitors may be a useful means of ameliorating the side effects of doxorubicin in patients undergoing chemotherapy.

MATERIALS AND METHODS

Gene Targeting. A 9-kb *Bam*H I fragment containing the *Cbr1* region from mouse chromosome 16 was cloned from PAC RPCI-21-82116 (13) into pBluescript (Stratagene, La Jolla, CA). Development of the hygromycin B resistance cassette of the vector has been described elsewhere.⁴ A 4.5-kb long arm of genomic sequence upstream of the *Cbr1* gene was isolated with *Xho*I and *Not*I restriction digestion. The *Xho*I site was blunted and cloned into the *Not*I and blunted *Bam*H I sites of the targeting vector polylinker. A 0.8-kb short arm of genomic sequence downstream of the *Cbr1* gene was isolated with *Apa*I and *Avr*II restriction digestion. The *Avr*II site was blunted, and *Apa*I linkers were used to clone the short arm into the *Apa*I site of the targeting vector.

MC1 embryonic stem cells were derived from 129S6/SvEv mice (Taconic, Germantown, NY) at the Johns Hopkins University Transgenic Core Facility⁵ and were cultured in 15% serum at 37°C under 5% CO₂. Linearized targeting vector (20 μg) was electroporated into 8 × 10⁶ MC1 cells at 0.32 kV and 250 μFarad using a Bio-Rad electroporator (Hercules, CA), and colonies were selected in 100 μg/ml hygromycin B (Invitrogen, Carlsbad, CA). Targeting was confirmed with genomic DNA Southern blot analysis (14) using random primed ³²P-labeled probes amplified with PCR primers Cbr14F (5' GGAGAGTTCCTGACAGACCA 3') and Cbr14R (5' CCACAGAGTATATGCCAGCT 3'), and Cbr15F (5' CTGAGCTCCCTGGTTCTCA 3') and Cbr15R (5' CAAGACCAAGACGACAGATG 3').

Twelve to 15 cells were injected into each of ~50 C57BL/6J blastocysts and transferred to five ICR surrogate mothers. Chimeric mice were bred to 129S6/SvEv (Taconic) females, and pups were typed by PCR primers CbrH2b (5' CACCTTCTTCTCAACCGTC 3') and CbrHR2 (5' CTCGTCCTGCAGTTCATCA 3') for the mutant allele and Cbr20F (5' CTGCTCCTTCTTCTGGGCTT 3') and Cbr20R (5' CTCACGGTATCTGGCTTCT 3') for the wild-type allele. PCR reactions contained 2 mM MgCl₂ and were performed for 30 cycles of denaturation (30 s 94°C), annealing (1 min 55°C), and extension (45 s 72°C).

Received 1/22/03; revised 7/17/03; accepted 7/18/03.

The costs of publication of this article were defrayed in part by the payment of page charges. This article must therefore be hereby marked *advertisement* in accordance with 18 U.S.C. Section 1734 solely to indicate this fact.

¹ Supported by USPHS award HD38384 (to R. H. R.). L. E. O. is supported on a Howard Hughes Predoctoral Fellowship. E. Rene Rodriguez provided support to D. B.

² To whom requests for reprints should be addressed, at Johns Hopkins University School of Medicine, Department of Physiology, 725 North Wolfe Street, Baltimore, MD 21205. Phone: (410) 955-6624; Fax: (410) 614-8731; E-mail: reeves@jhmi.edu.

³ The abbreviations used are: CBR1, carbonyl reductase 1; LVPW, left ventricular posterior wall; LVEDD, left ventricular end diastolic dimension; LVESD, left ventricular end systolic dimension.

⁴ J. T. Richtsmeier, J. S. Lund, E. S. Lindsay, J. Leszl, and R. H. Reeves. Mice homozygous for a null allele of *Gsc1* show dysmorphology of the cranial base and face. Submitted for publication.

⁵ M. Cowan, unpublished observations.

The *Cbr1* null allele was maintained on the 129S6/SvEv inbred background. The *Cbr1* null allele was also established on a C57BL/6J background (The Jackson Laboratory, Bar Harbor, ME) by more than seven generations of repeated backcrossing to produce B6.129-*Cbr1*^{tm1Rhr} mice.

Mice. Mice were maintained in a virus antibody-free colony, and given breeder chow and water *ad libitum*. They were injected once i.p. at 20 mg/kg with 1 mg/ml doxorubicin (Sigma Chemical Co., St. Louis, MO) in saline (Quality Biological, Inc., Gaithersburg, MD), observed and weighed daily. Animals were sacrificed when they exhibited distress and/or when weight loss approached 25%. All of the procedures were approved by the Institutional Animal Care and Use Committee.

Real-Time PCR. RNA was isolated from mouse tissues using the phenol solution Trizol (Invitrogen) and converted to cDNA using Superscript II RNase H⁻ Reverse Transcriptase (Invitrogen). *Cbr1* transcript levels were quantitated using LightCycler FastStart DNA Master SYBR Green I (Roche, Indianapolis, IN) with primers *Cbr1*Ex1F3 (5' GGTGCTAACAAAGGAATC 3') and *Cbr1*Ex2R2 (5' CTCTGCTTGAATGTGGAA 3'), and normalized to glyceraldehyde-3-phosphate dehydrogenase using primers *Gapdh*F2 (5' TGCATCTGCACCACCAACT 3') and *Gapdh*R2 (5' TGCCTGCTTACCACCTTC 3'). PCR reactions were carried out as suggested by the manufacturer with 3 mM MgCl₂ and an annealing temperature of 55°C.

Western Blotting. Mouse organs were homogenized in three volumes of ice-cold modified radioimmunoprecipitation assay buffer [50 mM Tris-HCl (pH 7.4), 1% NP40, 0.25% sodium deoxycholate, 150 mM NaCl, and 1 mM EDTA] containing protease inhibitor mixture (Sigma) diluted 1:60. Homogenates were centrifuged at 11,000 rpm for 10 min at 4°C and protein concentration in the supernatant was assayed with the DC Protein Assay kit (Bio-Rad). Five µg protein was separated by SDS-PAGE and blotted using standard protocols (14) using rabbit IgG antibody against recombinant human carbonyl reductase (6) kindly provided by Akira Hara (Gifu Pharmaceutical University, Gifu, Japan). Horseradish peroxidase-linked antirabbit immunoglobulin from donkey (Amersham Biosciences, Piscataway, NJ) was used as a secondary antibody. Mouse monoclonal antibody to α tubulin (Oncogene Research Products, San Diego, CA) and horseradish peroxidase-linked antimouse immunoglobulin from goat (Santa Cruz Biotechnology, Santa Cruz Biotechnology, CA) were used for loading controls. Bands were detected using the ECL Plus Western Blotting Detection kit (Amersham Biosciences), quantitated by densitometry using the α Imager system (α Innotech, San Leandro, CA), and normalized to tubulin. Ratios of expression in heterozygotes and wild-type were averaged from 2 animals per genotype.

High-Performance Liquid Chromatography Detection of Doxorubicin and Doxorubicinol. Plasma samples were prepared from whole blood collected from the saphenous vein (15) into heparinized micro-hematocrit capillary tubes (VWR, West Chester, PA) and centrifuged in Monoject Samplette capillary plasma separators (Mercedes Medical, Sarasota, FL) for 10 min at 2000 × g at 4°C. The plasma was removed and stored at -20°C. To extract samples, 100 µl of plasma was mixed with 900 µl of methanol:chloroform (3:2). Heart tissue was dried of surface moisture, weighed, and homogenized in 10 volumes of methanol:chloroform (3:2). The mixture was centrifuged at 3000 rpm for 10 min at room temperature, and the organic phase was vacuum extracted at 45°C under a stream of nitrogen. The residue was resuspended in 75 µl of acidified water, and 25 µl acetonitrile:tetrahydrofuran (40:1) was added. Aliquots of 50 µl were injected on the column.

The chromatographic separation was carried out on an ESA (Chelmsford, MA) high-performance liquid chromatography system with fluorescence detection. Samples were separated on a Waters (Milford, MA) Symmetry C₈ column (3.9 mm i.d. × 15 cm; 5 µm particle size), and doxorubicin and doxorubicinol were detected at an excitation wavelength of 480 nm and an emission wavelength of 560 nm. The mobile phase consisted of water:acetonitrile:tetrahydrofuran (75:25:0.4) with the pH adjusted to 2.0 with perchloric acid (16). The flow rate was set to 0.5 ml/min and run at room temperature. Plasma levels of each analyte were determined from values derived from spiked plasma standard curves using the ESA peak integration software followed by correction for dilution. Doxorubicinol standard was kindly provided by Farmitalia (Milan, Italy).

Cardiac Assessment. Echocardiography was performed initially on mice exhibiting a 10% decrease in body weight, with follow-up examinations two to three times a week to additionally monitor cardiac function. Mice were habituated to handling to prevent stress that may have occurred during the

experiment. To perform echocardiography on conscious animals (17), mice were gently held in supine position in the palm of the hand. The left hemithorax was shaved and a 1–2 mm-thick layer of prewarmed hypoallergenic ultrasonic transmission gel (Parker Laboratories, Fairfield, New Jersey) was applied to the thorax.

Transthoracic echocardiography was performed using a Hewlett-Packard Sono 5500 ultrasound machine with the 15MHz transducer. Images were stored on magnetic optical disk of 1.2 GB (Hewlett Packard) and T120 VHS tape. Two-dimensional and left ventricle M-mode measurements were taken in two separate 3–4-min sessions. The heart was first imaged in the two-dimensional mode in the parasternal short axis view at sweep speed of 150 mm/s. From this mode, an M-mode cursor was positioned perpendicular to the inter-ventricular septum and the LVPW at the level of the papillary muscles. From the M-mode, the left ventricular wall thickness and chamber dimensions were measured.

Image Analysis. All of the measurements were performed using the leading-edge method, as recommended by the American Society of Echocardiography (18). For each mouse, three to five values for each measurement were obtained and averaged for evaluation. Two research technologists trained in cardiac echocardiography performed the studies. Each operator was blinded to the experimental groups. The LVEDD, LVESD, interventricular septal wall thickness at end diastole, and LVPW thickness at end diastole were measured from the M-mode tracing. LV fractional shortening, the percent change in LV cavity dimensions, was calculated using the following equation: fractional shortening (%) = [(LVEDD - LVESD)/LVEDD] × 100. Ejection fraction represents stroke volume as a percentage of end diastolic LV volume and was calculated from the following equation: ejection fraction (%) = [(LVEDD² - LVESD²)/LVEDD²] × 100. The heart rate was determined by counting the diastole and systole cycles during M-mode imaging within a defined time interval and multiplying by the correction factor to obtain heartbeats per min.

Histopathology. Cardiac histopathology was assessed in each treatment group based on the method of Billingham (19) and modified by Gabrielson *et al.* (20). The hearts were fixed in phosphate-buffered 10% formalin, embedded in paraffin, sectioned at a thickness of 5 µm, and stained with H&E. The frequency and severity of myocardial lesions induced by doxorubicin was assessed by light microscopic examination. The changes were graded on the basis of the number of cardiomyocytes showing necrosis, mineralization, and cytoplasmic vacuolization.

Statistical Analysis. Transcript levels were analyzed using Student's *t* test. Doxorubicinol:doxorubicin ratios were analyzed using a one-tailed Wilcoxon rank sum test. Differences between strains for the echocardiographic data were investigated using a general linear model. To account for multiple comparisons, statistical differences between strains were calculated using the least significant difference test of PROC GLM in SAS version 8.02 (Cary, NC).

RESULTS

Creation of the *Cbr1* Null Allele. The targeting vector was designed to remove all three exons of the *Cbr1* gene. After transfection of the targeting vector, 120 hygromycin-resistant embryonic stem cell lines were screened by PCR and genomic Southern blotting. A single line was confirmed to have undergone homologous recombination at the *Cbr1* locus (Fig. 1A). This clone was injected into blastocysts, and the resulting chimeric mice were bred and progeny selected for germ-line transmission. 129-*Cbr1*^{tm1Rhr} mice were established by mating male chimeras directly to 129S6/SvEvTac females. All of the experiments reported here were performed in the 129 strain background. Homozygous null animals were never recovered from intercrosses of heterozygous (*Cbr1* +/-) mice, indicating that the null condition is fetal lethal. However, heterozygous mice are viable, fertile, and healthy.

Decreased *Cbr1* Transcript and Protein Levels, and Decreased Conversion of Doxorubicin to Doxorubicinol in Heterozygous Mice. We quantified *Cbr1* transcript levels using real-time PCR in heart (*n* = 4 *Cbr1* +/-, 7 +/+), liver (*n* = 3 +/-, 4 +/+), and kidney (*n* = 4 +/-, 4 +/+). *Cbr1* transcript levels were similar in

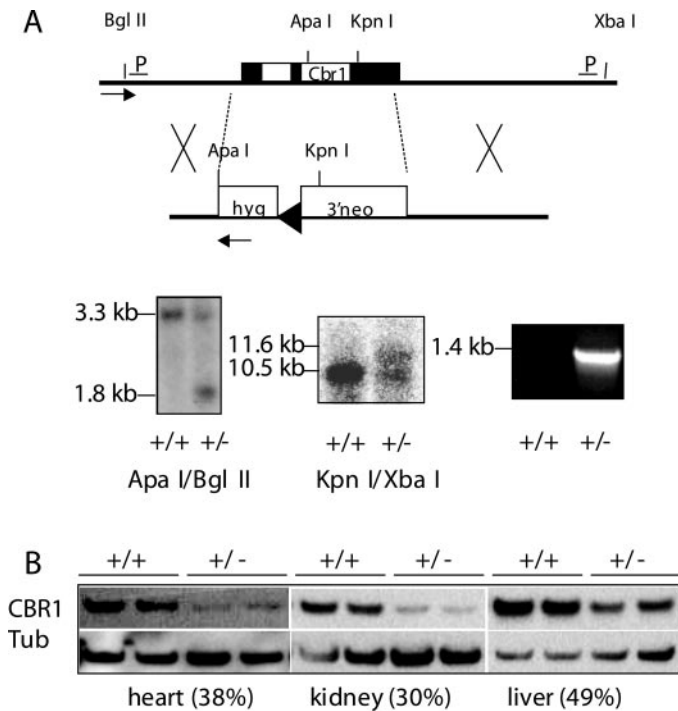


Fig. 1. Gene targeting to create a null allele of *Cbr1* in embryonic stem cells. The targeting vector (A) contained a hygromycin resistance gene (*hyg*), a loxP site (\blacktriangle), and the coding sequence of a neomycin resistance gene (3' *neo*), and removed all three exons (\blacksquare) of the *Cbr1* gene (not to scale). The endogenous allele yielded a 3.3-kb restriction fragment after digestion with *Apa*I and *Bgl*II, whereas the targeted allele was 1.8 kb. After digestion with *Kpn*I and *Xba*I, the endogenous allele was 10.5 kb, and the targeted allele was 1.4 kb; location of probes is designated (P). PCR primers (arrows) located outside the genomic targeting arm and within the vector yielded a 1.4-kb product only in a properly targeted cell line. The null allele resulted in lower CBR1 protein levels (B) in the heart, kidney, and liver. The percentage of wild-type CBR1 levels found in heterozygotes is shown in parentheses (see "Materials and Methods"). α -Tubulin (*Tub*) is shown as a loading control.

these organs ($\sim 10,000$ -fold less than control glyceraldehyde-3-phosphate dehydrogenase transcript levels) and were decreased in *Cbr1* +/- mice by 60% (heart, $P < 0.05$), 43% (liver, $P < 0.09$), and 65% (kidney, $P < 0.02$) relative to wild-type mice. This decrease was confirmed at the protein level by Western blotting (Fig. 1B).

The effect of decreased CBR1 protein levels on enzyme activity was reflected in plasma levels of doxorubicin and its metabolite, doxorubicinol, after i.p. injection of 20 mg/kg of the parent compound. Four h after administration, *Cbr1* +/- mice exhibited a lower conversion to doxorubicinol than did wild-type mice. Doxorubicinol: doxorubicin ratios were 0.23 ($1.85 \pm 0.05 \mu\text{g/ml}:7.90 \pm 0.10 \mu\text{g/ml}$) and 0.59 ($3.25 \pm 0.60 \mu\text{g/ml}:5.53 \pm 0.56 \mu\text{g/ml}$) in *Cbr1* +/- and wild-type mice, respectively ($P < 0.067$; $n = 2$ *Cbr1* +/-, 4 +/+). Significant differences were not observed at 12 h ($n = 4$ *Cbr1* +/-, 2 +/+) or 24 h ($n = 2$ *Cbr1* +/-, 4 +/+) after administration. We also assayed doxorubicin and doxorubicinol levels in the heart at three time points (4 h, $n = 2$ *Cbr1* +/-, 4 +/+, 12 h, $n = 4$ *Cbr1* +/-, 2 +/+, 24 h $n = 2$ *Cbr1* +/-, 3 +/). No differences were detected. Doxorubicin levels in heart ranged from 0.7 to 23.7 $\mu\text{g/ml}$; doxorubicinol levels were all below 0.7 $\mu\text{g/ml}$ and in most cases were undetectable in heart.

Protection from Doxorubicin-Induced Weight Loss and Death in *Cbr1* +/- Mice. To determine whether a decrease in CBR1 was protective against doxorubicin-induced cardiotoxicity, 11 *Cbr1* +/- mice and 11 wild-type controls were given a single i.p. injection of 20 mg/kg doxorubicin. Mice were weighed daily and observed for signs of weakness. After an initial weight loss, *Cbr1* heterozygotes stabilized, whereas control animals continued to lose weight (Fig. 2).

Wild-type mice exhibited lethargy and 3–5°C lower body temperature. When the experiment was terminated 18 days after doxorubicin injection, 91% of wild-type mice had died or were euthanized because of distress or weight loss compared with 18% of heterozygous *Cbr1* knockout mice (Fig. 3).

Echocardiographic Assessment of Doxorubicin-Treated Mice. Cardiac function was examined noninvasively in doxorubicin-treated mice *in vivo* using transthoracic echocardiography. Wild-type mice were severely bradycardic and exhibited global dilation of the left ventricle in end diastole and systole (Fig. 4). Thinning of the LVPWs and interventricular septal walls in addition to a significant decrease in fractional shortening and ejection fraction were common features of this doxorubicin-induced cardiomyopathy (Table 1). *Cbr1* +/- mice were protected from these changes and were equivalent to untreated controls at a statistically significant level for all of the manifestations (F statistic > 8.57 ; $P < 0.002$). Because untreated *Cbr1* +/- and wild-type mice showed no differences in echocardiographic parameters, data from both groups were combined for the purpose of comparison with treated animals.

Histopathological Analysis of Doxorubicin-Treated Mouse Hearts. Treated mice were euthanized after exhibiting distress or weight loss approaching 25% of initial body weight. All of the surviving mice were sacrificed at 18 days, and hearts were prepared for histological analysis. Extensive necrosis and mineralization of cardiomyocytes combined with a mild degree of cardiomyocyte vacuolation were observed in doxorubicin-treated wild-type mouse hearts. *Cbr1* +/- mice showed little evidence of cardiomyocyte pathological changes (Fig. 5).

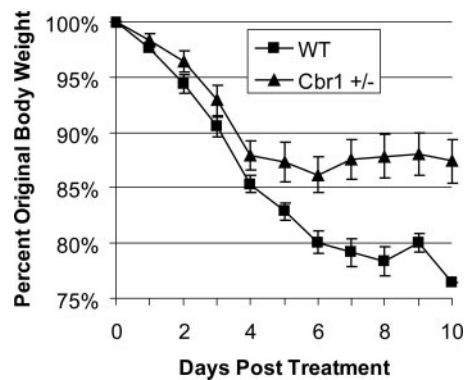


Fig. 2. Loss of one copy of *Cbr1* inhibits weight loss in doxorubicin-treated mice. Wild-type (\blacksquare , $n = 11$) and *Cbr1* +/- (\blacktriangle , $n = 11$) mice were injected i.p. with 20 mg/kg doxorubicin and weighed daily. The mean weight of surviving mice is shown as percentage of the pretreatment weight; bars, \pm SE. The day 10 wild-type data point shows the percentage of original weight of the only surviving animal of that genotype.

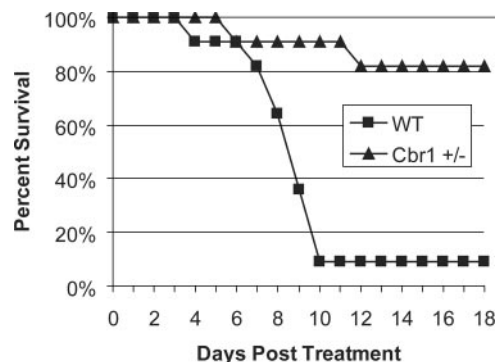
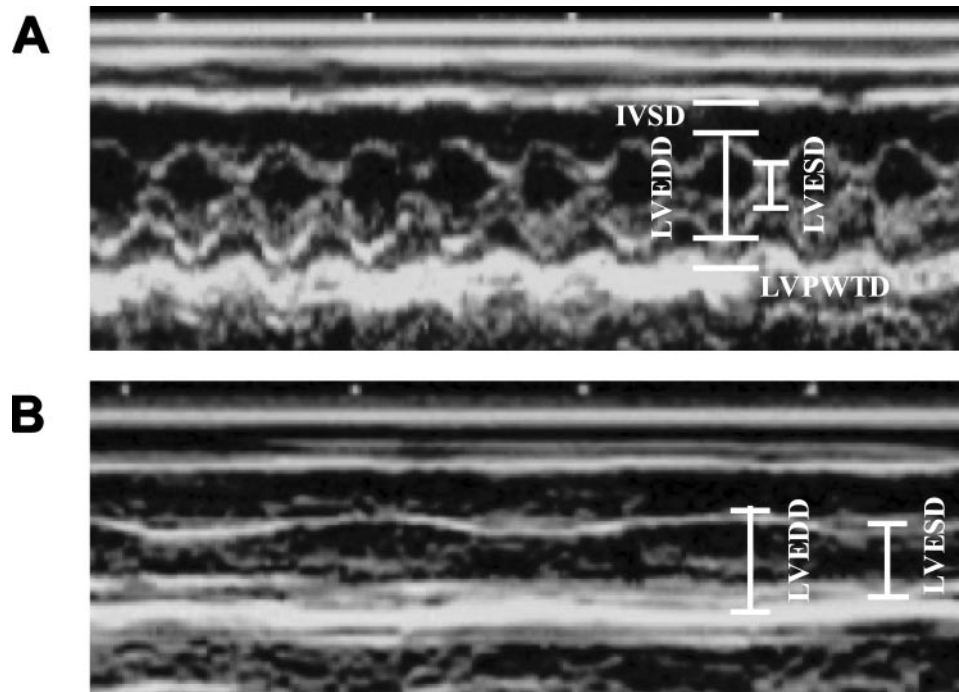


Fig. 3. *Cbr1* +/- mice are protected against mortality after doxorubicin treatment. After 18 days, 10 of 11 wild type mice (\blacksquare) as compared with 2 of 11 *Cbr1* +/- mice (\blacktriangle) had died or had been euthanized because of distress or weight loss.

Fig. 4. Doxorubicin treatment induces cardiac function deficits in wild-type but not in *Cbr1* +/- mice. Transthoracic echocardiograms of conscious doxorubicin-treated *Cbr1* +/- (A) and wild-type (B) mice were obtained *in vivo*. The figure represents a motion mode of the left ventricle, which is obtained with a single ultrasound beam transmitted through the heart with the resulting image displayed over time. In this image the frame is -0.8 s. Wild-type mice exhibited a decreased heart rate and global dilation of the left ventricle with low contractility. *LVEDD*, left ventricular end diastolic dimension; *LVESD*, left ventricular end systolic dimension; *IVSD*, interventricular septal wall thickness at end diastole; *LVPWTD*, left ventricular posterior wall thickness at end diastole.



DISCUSSION

Loss of one copy of *Cbr1* decreases levels of the protein and is sufficient to protect mice from cardiotoxicity induced by doxorubicin treatment. This cardiac protection is likely because of the decreased enzymatic conversion of doxorubicin to its metabolite, doxorubicinol, which is believed to be responsible for heart damage in patients treated with this highly effective anticancer drug. The conversion of doxorubicin can occur in both the liver and heart, with greater accumulation of doxorubicinol in the myocardium (21–23). CBR1 has been shown to be the major reductase in mouse kidney, spleen, and heart (6). Enzymes that reduce carbonyls include carbonyl reductases, aldehyde reductases, aldose reductases, and dihydrodiol dehydrogenases (24, 25). These enzymes have overlapping substrate specificities including many endogenous and xenobiotic compounds. However, these activities did not compensate for the loss of a *Cbr1* allele. Our results validate the potential of pharmacological targeting of CBR1 as a prophylactic in conjunction with doxorubicin treatment.

Doxorubicinol is thought to be responsible for cardiotoxicity but not for chemotherapeutic efficacy of doxorubicin chemotherapy (4), so the pharmacologic inhibition of CBR1 may be cardioprotective without a loss of potency. The antineoplastic effects of doxorubicin appear to be primarily because of its effects in dividing cells that are sensitive to topoisomerase II inhibition, DNA intercalation, and RNA synthesis inhibition (26). The inhibition of carbonyl reductase with pharmacological inhibitors should result in an increase in tumor exposure to the parent chemotherapeutic compound, doxorubicin, with a concurrent decrease in cardiac exposure to the CBR1 metabolite, doxorubicinol. Our results indicate that it would not be necessary to completely abolish CBR1 activity, because significant protection is seen in heterozygous mice with a 40–50% decrease of CBR1 protein levels.

Inhibition of carbonyl reductase activity may be a more effective prophylactic than other cardioprotective agents. Antioxidants such as vitamin E and ascorbic acid have been tested and proven ineffective to date (3). Of the few cardioprotective agents available, dexrazoxane is the best studied in animal models (27). This iron chelator has some efficacy in decreasing doxorubicin-induced cardiac toxicity. Unfortu-

nately, chelating iron is neither specific nor complete in its cardioprotective effects. In addition, dexrazoxane affects the pharmacokinetics of doxorubicin, and this in some cases decreases the effective antineoplastic dose (2, 3). Dexrazoxane also has its own side effects, because it is toxic to hematopoietic cells and may cause chemical phlebitis (28).

The responses to pharmacological agents in the human population are highly variable, owing in part to genetic variation in the population (29). In preliminary experiments, the protective effect of decreasing *Cbr1* levels that we report here for 129-*Cbr1* +/- mice was not seen when the null allele was bred onto the C57BL/6J genetic background. This difference may provide a means for isolating the modifier genes that are responsible. Ultimately, an understanding of variation in the human orthologues of these genes could provide important insights into the most efficacious use of doxorubicin in human beings.

The human *CBR1* gene is found on chromosome 21, and, thus, is present in three copies in individuals with Down syndrome. *CBR1* mRNA is present at elevated levels in Down syndrome cells (30), and may contribute to the increased toxicity of chemotherapy reported in patients with Down syndrome (31). The development of a CBR1 inhibition therapy could be especially beneficial to individuals with Down syndrome.

Table 1 Echocardiographic measurements in doxorubicin-treated mice

Measurements shown are matched from 6–9 days after injection. *Cbr1* +/- mice are different from +/+ mice and equivalent to untreated controls at a statistically significant level for all manifestations ($P < 0.002$). Mean values \pm SE are shown. *Cbr1* +/- mice were still equivalent to controls at 15 days after injection ($P < 0.004$) after most +/- mice had died. Untreated control data include combined data from both genotypes. *LVEDD*, left ventricular end diastolic dimension; *LVESD*, left ventricular end systolic dimension; *IVSD*, interventricular septal wall thickness at end diastole; *LVPWTD*, left ventricular posterior wall thickness at end diastole; *FS*, fractional shortening; *EF*, ejection fraction; *HR*, heart rate.

	<i>Cbr1</i> +/+ ($n = 7$)	<i>Cbr1</i> +/- ($n = 8$)	Untreated ($n = 8$)
<i>LVEDD</i> (mm)	3.40 \pm 0.10	2.74 \pm 0.08	2.96 \pm 0.03
<i>LVESD</i> (mm)	2.06 \pm 0.16	1.07 \pm 0.08	1.03 \pm 0.01
<i>IVSD</i> (mm)	0.55 \pm 0.07	0.76 \pm 0.06	0.86 \pm 0.01
<i>LVPWTD</i> (mm)	0.51 \pm 0.05	0.78 \pm 0.06	0.86 \pm 0.01
<i>FS</i> (%)	39.7 \pm 3.8	60.6 \pm 3.4	65.2 \pm 0.2
<i>EF</i> (%)	62.9 \pm 4.0	83.9 \pm 3.2	87.9 \pm 0.1
<i>HR</i> (beats/min)	343 \pm 61	649 \pm 16	656 \pm 3

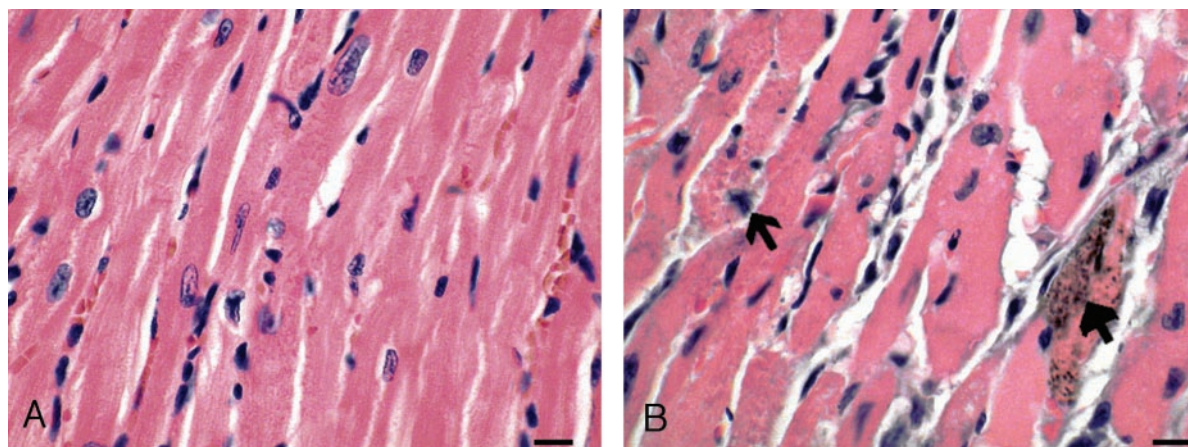


Fig. 5. *Cbr1* +/- mouse hearts are protected from doxorubicin-induced injury. In A, the organized pattern of myofiber striations with central nuclei, as expected in untreated mice, are observed in doxorubicin-treated *Cbr1* +/- mice. In B, doxorubicin treatment, in contrast, produced necrosis (open arrow) and mineralization (filled arrow) in wild-type mice. Sections were stained with H&E. Bar = 20 μ m.

The first reports of doxorubicin-induced cardiotoxicity were published 30 years ago (32). We hope that the use of a mouse model to confirm a target for rational drug design, as reported here, may speed the discovery of small molecule therapeutics to ameliorate the side effects of this otherwise highly effective chemotherapeutic agent.

ACKNOWLEDGMENTS

We thank Mitra Cowan for embryonic stem cells and Dr. Wendy Kimber for contributions to the construction of the *Cbr1* targeting vector. Dr. Randall Roper assisted with statistical analysis. Dr. Akira Hara kindly provided antibody for detection of CBR1 protein.

REFERENCES

- Singal, P. K., and Iliskovic, N. Doxorubicin-induced cardiomyopathy. *N. Engl. J. Med.*, 339: 900–905, 1998.
- Gharib, M. I., and Burnett, A. K. Chemotherapy-induced cardiotoxicity: current practice and prospects of prophylaxis. *Eur. J. Heart Fail.*, 4: 235–242, 2002.
- Wojtacki, J., Lewicka-Nowak, E., and Lesniewski-Kmak, K. Anthracycline-induced cardiotoxicity: clinical course, risk factors, pathogenesis, detection and prevention—review of the literature. *Med. Sci. Monit.*, 6: 411–420, 2000.
- Mordente, A., Meucci, E., Martorana, G. E., Giardina, B., and Minotti, G. Human heart cytosolic reductases and anthracycline cardiotoxicity. *IUBMB Life*, 52: 83–88, 2001.
- Forrest, G. L., and Gonzalez, B. Carbonyl reductase. *Chem. Biol. Interact.*, 129: 21–40, 2000.
- Ishikura, S., Yamamoto, Y., Matsuura, K., Wei, J., Hodes, M. E., and Hara, A. Properties and tissue distribution of mouse monomeric carbonyl reductase. *Biol. Pharm. Bull.*, 21: 879–881, 1998.
- Watanabe, K., Sugawara, C., Ono, A., Fukuzumi, Y., Itakura, S., Yamazaki, M., Tashiro, H., Osoegawa, K., Soeda, E., and Nomura, T. Mapping of a novel human carbonyl reductase, CBR3, and ribosomal pseudogenes to human chromosome 21q22.2. *Genomics*, 52: 95–100, 1998.
- Reymond, A., Marigo, V., Yaylaoglu, M. B., Leoni, A., Ucla, C., Scamuffa, N., Caccioppoli, C., Dermitzakis, E. T., Lyle, R., Banfi, S., Eichele, G., Antonarakis, S. E., and Ballabio, A. Human chromosome 21 gene expression atlas in the mouse. *Nature (Lond.)*, 420: 582–586, 2002.
- Gitton, Y., Dahmane, N., Baik, S., Ruiz i Altaba, A., Neidhardt, L., Scholze, M., Herrmann, B. G., Kahlem, P., Benkahl, A., Schrinner, S., Yildirimman, R., Herwig, R., Lehrach, H., and Yaspo, M. L. A gene expression map of human chromosome 21 orthologues in the mouse. *Nature (Lond.)*, 420: 586–590, 2002.
- Wei, J., Dlouhy, S. R., Hara, A., Ghetti, B., and Hodes, M. E. Cloning a cDNA for carbonyl reductase (Cbr) from mouse cerebellum: murine genes that express cbr map to chromosomes 16 and 11. *Genomics*, 34: 147–148, 1996.
- Licata, S., Saponiero, A., Mordente, A., and Minotti, G. Doxorubicin metabolism and toxicity in human myocardium: role of cytoplasmic deglycosidation and carbonyl reduction. *Chem. Res. Toxicol.*, 13: 414–420, 2000.
- Forrest, G. L., Gonzalez, B., Tseng, W., Li, X., and Mann, J. Human carbonyl reductase overexpression in the heart advances the development of doxorubicin-induced cardiotoxicity in transgenic mice. *Cancer Res.*, 60: 5158–5164, 2000.
- Pletcher, M. T., Wiltshire, T., Cabin, D. E., Villanueva, M., and Reeves, R. H. Use of comparative physical and sequence mapping to annotate mouse chromosome 16 and human chromosome 21. *Genomics*, 74: 45–54, 2001.
- Ausubel, F. M., Brent, R., Kingston, R. E., Moore, D. D., Seidman, J. G., Smith, J. A., and Struhl, K. *Current Protocols in Molecular Biology*, Vol. 1, pp. 2.9.1–2.10.3. Hoboken, New Jersey: John Wiley & Sons, Inc., 1995.
- Hem, A., Smith, A. J., and Solberg, P. Saphenous vein puncture for blood sampling of the mouse, rat, hamster, gerbil, guinea pig, ferret and mink. *Lab. Anim.*, 32: 364–368, 1998.
- de Bruijn, P., Verweij, J., Loos, W. J., Kolker, H. J., Planting, A. S., Nooter, K., Stoter, G., and Sparreboom, A. Determination of doxorubicin and doxorubicinol in plasma of cancer patients by high-performance liquid chromatography. *Anal. Biochem.*, 266: 216–221, 1999.
- Yang, X. P., Liu, Y. H., Rhaleb, N. E., Kurihara, N., Kim, H. E., and Carretero, O. A. Echocardiographic assessment of cardiac function in conscious and anesthetized mice. *Am. J. Physiol.*, 277: H1967–H1974, 1999.
- Sahn, D. J., DeMaria, A., Kisslo, J., and Weyman, A. Recommendations regarding quantitation in M-mode echocardiography: results of a survey of echocardiographic measurements. *Circulation*, 58: 1072–1083, 1978.
- Billingham, M. Role of endomyocardial biopsy in diagnosis and treatment of heart disease. In: M. D. Silver (ed.), *Cardiovascular Pathology*, Ed. 2, pp. 1465–1486. New York: Churchill Livingstone, 1991.
- Gabrielson, K. L., Hogue, B. A., Bohr, V. A., Cardounel, A. J., Nakajima, W., Kofler, J., Zweier, J. L., Rodriguez, E. R., Martin, L. J., de Souza-Pinto, N. C., and Bressler, J. Mitochondrial toxin 3-nitropropionic acid induces cardiac and neurotoxicity differentially in mice. *Am. J. Pathol.*, 159: 1507–1520, 2001.
- Carter, S. K. Adriamycin—a review. *J. Natl. Cancer Inst.*, 55: 1265–1274, 1975.
- Del Tacca, M., Danesi, R., Ducci, M., Bernardini, C., and Rominini, A. Might adriamycinol contribute to adriamycin-induced cardiotoxicity? *Pharmacol. Res. Commun.*, 17: 1073–1084, 1985.
- Olson, R. D., Mushlin, P. S., Brenner, D. E., Fleischer, S., Cusack, B. J., Chang, B. K., and Boucek, R. J., Jr. Doxorubicin cardiotoxicity may be caused by its metabolite, doxorubicinol. *Proc. Natl. Acad. Sci. USA*, 85: 3585–3589, 1988.
- Oppermann, U. C., and Maser, E. Molecular and structural aspects of xenobiotic carbonyl metabolizing enzymes. Role of reductases and dehydrogenases in xenobiotic phase I reactions. *Toxicology*, 144: 71–81, 2000.
- Oppermann, U. C., Filling, C., and Jornvall, H. Forms and functions of human SDR enzymes. *Chem. Biol. Interact.*, 130–132: 699–705, 2001.
- Chabner, B. A., Allegra, C. J., Curt, G. A., and Calabresi, P. *Antineoplastic Agents*. In: J. G. Hardman and L. E. Limbird (eds.), *Goodman & Gilman's The Pharmacological Basis of Therapeutics*, Ed. 9, pp. 1233–1288. New York: McGraw-Hill Professional, 1996.
- Herman, E. H., and Ferrans, V. J. Preclinical animal models of cardiac protection from anthracycline-induced cardiotoxicity. *Semin. Oncol.*, 25: 15–21, 1998.
- Hoekman, K., van der Vijgh, W. J., and Vermorken, J. B. Clinical and preclinical modulation of chemotherapy-induced toxicity in patients with cancer. *Drugs*, 57: 133–155, 1999.
- Kuehl, P., Zhang, J., Lin, Y., Lamba, J., Assem, M., Schuetz, J., Watkins, P. B., Daly, A., Wrighton, S. A., Hall, S. D., Maurel, P., Relling, M., Brimer, C., Yasuda, K., Venkataraman, R., Strom, S., Thummel, K., Boguski, M. S., and Schuetz, E. Sequence diversity in CYP3A promoters and characterization of the genetic basis of polymorphic CYP3A5 expression. *Nat. Genet.*, 27: 383–391, 2001.
- Lemieux, N., Malfoy, B., and Forrest, G. L. Human carbonyl reductase (CBR) localized to band 21q22.1 by high-resolution fluorescence *in situ* hybridization displays gene dosage effects in trisomy 21 cells. *Genomics*, 15: 169–172, 1993.
- Lange, B. J., Kobrinsky, N., Barnard, D. R., Arthur, D. C., Buckley, J. D., Howells, W. B., Gold, S., Sanders, J., Neudorf, S., Smith, F. O., and Woods, W. G. Distinctive demography, biology, and outcome of acute myeloid leukemia and myelodysplastic syndrome in children with Down syndrome: Children's Cancer Group Studies 2861 and 2891. *Blood*, 91: 608–615, 1998.
- Lefrak, E. A., Pitha, J., Rosenheim, S., and Gottlieb, J. A. A clinicopathologic analysis of adriamycin cardiotoxicity. *Cancer (Phila.)*, 32: 302–314, 1973.